

ARTICLE

Position-dependent hexaarylbenzene AIEgens: synthesis, characterization and optical properties

Received 00th January 20xx,
Accepted 00th January 20xx

Wen-Xuan Zhao,^a Li-Feng Yang,^b Dan Yu,^b Fei-Yu Chen,^b Ling Liang,^a Jing-Yi Cao,^a Guang Yang,^a Shu-Hai Chen,^a Takehiko Yamato,^{*c} Carl Redshaw^d and Chuan-Zeng Wang,^{*a}

DOI: 10.1039/x0xx00000x

With the development and exploration of photoelectric materials, the design of tunable and high luminescence efficiency materials remains a challenge. As a promising candidate, AIE luminogens have shown significant advantages. Herein, two tetraphenylethene-fused hexaarylbenzene derivatives with strong electron-withdrawing groups (–CN) were synthesized. Both compounds exhibit obvious AIE-active properties with reasonable $\alpha_{\text{AIE}} = I_{\text{water}} (I_{\text{water}} = 99\%) / I_{\text{THF}}$ (51.7 for **p-TPE-HAB** and 9 for **o-TPE-HAB**). **p-TPE-HAB**, and high photoluminescence quantum yields were recorded to be 62.8% for **p-TPE-HAB** and 35.3% for **o-TPE-HAB**). The position-dependent emission behavior indicates that this hybridization strategy may be used for the design and fabrication of AIEgens with tunable and controllable photophysical properties.

Introduction

In the past two decades, luminogens with aggregation-induced emission (AIE) attributes have received extensive attention and seen rapid development due to their outstanding advantages in chemosensing, bioimaging, optoelectronics, and stimuli-responsive systems.^{1–4} The family of AIE luminogens (AIEgens) is constantly growing with the synthesis of multiple types of AIE systems, such as small molecular AIEgens,⁵ AIE co-crystals,^{6,7} AIE polymers,^{8–10} and metal-complex AIEgens.^{11–13} Small molecular AIEgens are still the focus in aggregate science due to their accurate and simple structures, interpretable luminescence mechanism and structure-property relationships.³ A series of prototypical AIEgens, including hexaphenylsilole (HPS),¹⁴ tetraphenylethene (TPE),¹⁵ and 10,10',11,11'-tetrahydro-5,5'-bidibenzo[a,d][7] annulenyliene (THBA),¹⁶ have opened up new avenues for the exploration of their wider potential by evading the notorious aggregation-caused quenching (ACQ) effect in the solid state. Subsequently, more types of AIEgens have been developed as building blocks for functional

materials, such as tetraphenylbenzene,¹⁷ tetraphenylpyrazine,¹⁸ polyarylpyrrole.¹⁹

For traditional luminophores, such as polycyclic aromatic hydrocarbons (PAHs), the ACQ effect is the biggest obstacle to the development of potential applications.²⁰ In this context, a more efficient and popular strategy was established by decorating the PAH core with an AIE unit, whereupon a reasonable luminescence efficiency is achieved both in solution and in the solid state.^{21,22} Moreover, the combination of different AIE units results in even more interesting and fascinating optical properties, such as mechanochromism, thermochromism, and chronochromism.^{23–25} Propeller-shaped AIEgens should be considered the most favored candidate because of the active intramolecular rotation in dilute solution and restricted motion in the aggregated state. The effect of rotational freedom on photophysical properties becomes an important feature for exploring the luminescence mechanisms in different aggregated states.²⁶

In the present work, a novel hybridization strategy combining intramolecular charge transfer (ICT) effect was performed, and two nonplanar AIEgens were designed by employing TPE and hexaphenylbenzene (HPB) building blocks (see **Scheme 1**). Meanwhile, the strong electron-withdrawing group (–CN) was also introduced as a charge-regulating group. The optical properties of these two AIEgens were systematically investigated by experimental and theoretical methods. The significant position-dependent emission behavior allows for interesting structure-property relationships that deepen our understanding of the mechanism.

^a School of Chemistry and Chemical Engineering, Shandong University of Technology, Zibo 255049, P. R. China. E-mail: czwang@sdu.edu.cn

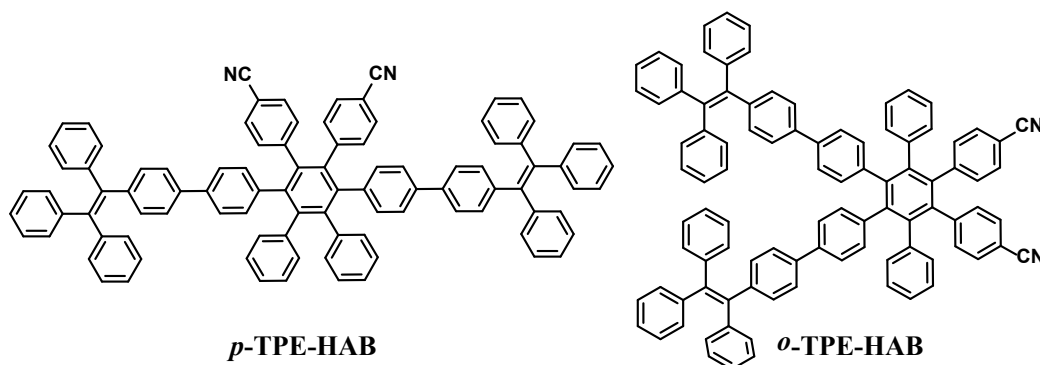
^b Shaoxing Sewage Treatment Development Co., Ltd, Xingbin Road, Keqiao District, Shaoxing, P. R. China.

^c Department of Applied Chemistry, Faculty of Science and Engineering, Saga University Honjo-machi 1, Saga 840-8502 Japan. E-mail: yamatot@cc.saga-u.ac.jp

^d Chemistry, School of Natural Sciences, The University of Hull, Cottingham Road, Hull, Yorkshire HU6 7RX, UK

† Footnotes relating to the title and/or authors should appear here.

Electronic Supplementary Information (ESI) available: [details of any supplementary information available should be included here]. See DOI: 10.1039/x0xx00000x



Scheme 1. Chemical structures of ***p*-TPE-HAB** and ***o*-TPE-HAB**.

Results and discussion

Synthesis and characterization

The synthetic procedures for the two AIEgens ***p*-TPE-HAB**, ***o*-TPE-HAB** and precursors are outlined in [Scheme S1](#). Firstly, formation of the HPB framework by a Diels-Alder reaction required the cyclopentadienone derivatives **3**. This in turn was synthesized by the base-catalyzed condensation of the benzil derivatives and dibenzyl ketone shown in the scheme. The Diels-Alder reaction of **3** and 4,4'-(ethyne-1,2-diyl)dibenzonitrile was followed by spontaneous loss of carbon monoxide²⁷ to give precursor **4** in good yield (> 80%) under reflux conditions. The synthesis of partial raw materials is shown in experimental section, and other reagents were obtained

commercially and were used without further purification. All compounds were characterized by ¹H and ¹³C-NMR spectroscopy, and high-resolution mass spectrometry ([Figs. S1–S7, ESI†](#)).

Photophysical properties

The photophysical properties of ***p*-TPE-HAB** and ***o*-TPE-HAB** in dilute solutions (THF) and in the solid are depicted in [Table 1](#). As shown in [Fig. 1](#), different emission behavior was observed with emission maxima centered at 402 nm for ***p*-TPE-HAB** and 387 nm for ***o*-TPE-HAB** in dilute THF solution. Both luminogens displayed an obvious red-shift compared with single component TPE ($\lambda_{em} = 350$ nm) and HPB ($\lambda_{em} = 334$ nm), respectively,²⁸ which may be attributed to the influence of the communication of both π -systems by the efficient energy and charge transfer from TPE moieties to the HAB core decorating with –CN groups.²⁹

Table 1. The photophysical properties of ***p*-TPE-HAB** and ***o*-TPE-HAB**.

Compounds	λ_{em} (nm) sol ^[a] /solid	Φ_{FL} ^[b] (%) sol ^[a] /solid	Φ_{FL} ^[c] (%)	HOMO ^[d] (eV)	LUMO ^[d] (eV)	ΔE_g ^[d] (eV)	α_{AIE} ^[e]
<i>p</i>-TPE-HAB	402 / 495	1.2 / 35.5	62.8	–5.30	–1.66	3.64	517
<i>o</i>-TPE-HAB	387 / 502	0.7 / 8.5	35.3	–5.33	–1.69	3.64	9

^a 1×10^{-7} M in CH₂Cl₂, λ_{em} is the fluorescence band appearing at the shortest wavelength; ^b Absolute quantum yield (± 0.01 – 0.03); ^c Absolute quantum yield in a water/THF mixed solvent system ($f_w = 99\%$); ^d DFT/B3LYP/6-31G* using Gaussian; ^e $\alpha_{AIE} = I_{f,water} (f_{water} = 99\%) / I_{THF}$.

Closer inspection of the emission spectra of the two luminogens in dilute THF solution reveals that the emission maximum of ***p*-TPE-HAB** ($\lambda_{em, max} = 402$) is red-shifted relative to ***o*-TPE-HAB** ($\lambda_{em, max} = 387$), which can be ascribed to the difference in the co-planarity in these two molecular systems due to the effects of the substituents.³⁰ In sharp contrast, distinct emission behavior was observed for these two luminogens in the solid state compared to dilute solution. A large red-shift of ***p*-TPE-HAB** at 495 nm and ***o*-TPE-HAB** at 502 nm was recorded, respectively. In general, the above-mentioned emission behavior with a significant red-shift can be attributed to the synergistic effect of through-space charge transfer (TSCT)^{31, 32} and the different molecular arrangements. The luminogen ***o*-TPE-HAB** exhibited a red-shift of 7 nm compared to ***p*-TPE-HAB** in the solid

state, which may be ascribed to a more significant TSCT effect in the ***o*-TPE-HAB** molecular system. Specifically, a shell-like intermolecular donor-acceptor (D-A) type behavior is presumed in the *ortho*-substituted molecular structures; two adjacent TPE groups of one molecule may hold a moiety of another molecule. The fluorescence quantum yields (Φ_{FL}) were measured in dilute solution and in the solid state. As shown in [Table 1](#), both luminogens exhibit low emission efficiency in dilute organic solution (1.2% for ***p*-TPE-HAB** and 0.7% for ***o*-TPE-HAB**, respectively). On the other hand, higher photoluminescence quantum yields were observed (35.5% for ***p*-TPE-HAB** and 8.5% for ***o*-TPE-HAB**), which is largely due to the restriction of intramolecular rotation (RIR) mechanism based on the twisted TPE and HPB units.

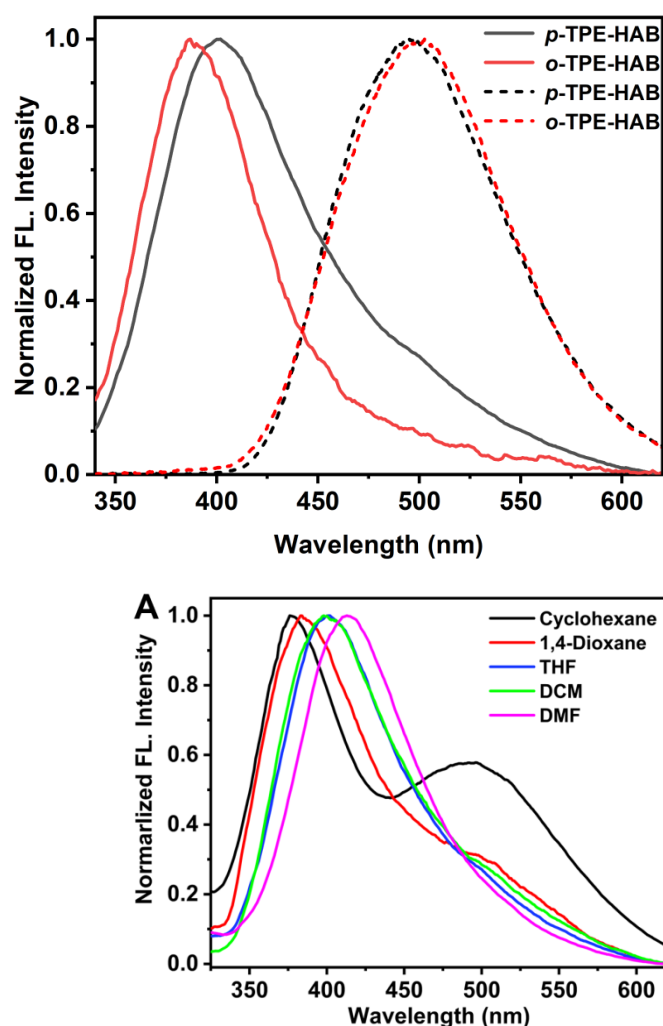


Fig. 2. Solvatochromism effect of emission spectra for *p*-TPE-HAB and *o*-TPE-HAB in solvents with varying polarity.

In view of the AIE characteristics of the TPE and HPB derivatives, further investigation of the emission behavior of *p*-TPE-HAB and *o*-TPE-HAB in their aggregated state was performed. Specifically, the emission behavior of *p*-TPE-HAB and *o*-TPE-HAB in THF/H₂O mixtures were recorded, and both molecules were unsurprisingly found to be AIE-active materials. As shown in Fig. 3A, the emission behavior of *o*-TPE-HAB in THF/H₂O mixtures exhibited a slight red-shift from 389 nm to 406 nm and quenching on increasing the water fraction (f_w) from 0% to 70%, which may be attributed to the increased solvent polarity.²¹ In the process of increasing water fraction from 70% to 99% or even higher, the emission intensity exhibits a rapid enhancement of approximately 9-fold ($\alpha_{\text{AIE}} = 9$), which is mainly attributed to the restriction of intramolecular rotation (RIR) mechanism.³⁴ Meanwhile, a small red-shift of maximum emission

wavelength was observed upon increasing the f_w from 0% to 70%, while a distinct red-shift from 408 nm to 501 nm was evident at the turning point $f_w = 80\%$. A slight blue-shift was recorded in water-dominated solutions ($90\% < f_w < 99\%$), which may be ascribed to the difference in the intermolecular interactions for the different aggregated states.^{35,36} On the other hand, the AIEgen *p*-TPE-HAB presents similar photophysical properties for the emission intensity and maximum emission wavelength (Fig. S8, ESI[†]). Moreover, *p*-TPE-HAB possesses a higher α_{AIE} value of 517, which can be attributed to the effects of the substituents. The results of both AIEgens are also consistent with the above mentioned photoluminescence quantum yields.

Fig. 1. Emission spectra (B) for luminogens *p*-TPE-HAB and *o*-TPE-HAB in THF solution (solid line) and in the solid state (dash line), respectively.

To further interpret the emission mechanism, a study of the solvatochromic effects in different organic solvents of various polarities (cyclohexane, 1,4-dioxane, tetrahydrofuran (THF), dichloromethane (DCM) and dimethylformamide (DMF)) was conducted. The solvatochromic effects for all compounds basically supported our interpretation of the ICT effect.³³ As shown in Fig. 2, the two luminogens exhibited similar emission behavior in different organic solvents, and dual emission properties were observed in low polarity solvents, while a singlet emission peak was recorded in high polarity solvents. Meanwhile, a red-shift of the maximum emission peak was observed. The almost identical value of the red-shift of the maximum emission peak (37 nm for *p*-TPE-HAB and 38 nm for *o*-TPE-HAB) on increasing the polarity can be attributed to the similar ICT effects in both molecular systems.

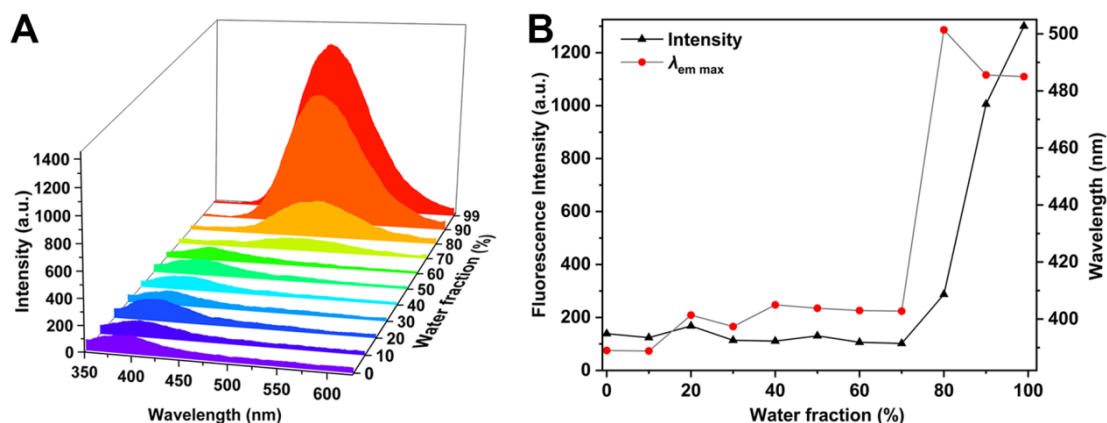


Fig. 3 (A) The fluorescence spectra of *o*-TPE-HAB in mixed H₂O/THF solutions (1 × 10⁻⁶ M); (B) Plots of maximum emission wavelength and emission intensity at different water fractions (0–99 vol%) for *o*-TPE-HAB.

Density functional theory (DFT) calculations were carried out to evaluate the structure-activity relationship of the position-dependent hexaarylbenzene AIEgens and the electron delocalization at the B3LYP/6-31G* level.^{37, 38} The energy levels and frontier-molecular-orbital distributions of their LUMO and HOMO are depicted in Fig. 4. For the AIEgens *p*-TPE-HAB and *o*-TPE-HAB, similar frontier-molecular-orbital distributions and energy levels, especially for energy gaps (ΔE_{g}), were observed, and the LUMOs are mainly localized on the central C6 ring and the strong electron-withdrawing –CN substituents of the phenyl groups. Meanwhile, the HOMOs are almost completely distributed over the entire TPE units. The separated HOMO and LUMO distribution for both AIEgens confirmed our previous interpretation of the solvatochromic effect and ICT behavior in this type of hexaarylbenzene AIEgens. All results including the theoretical and experimental data indicate that this type of AIEgens exhibits competitive and tunable photophysical properties, such as luminescence efficiency, and are white-light emitting materials with dual emission bands.

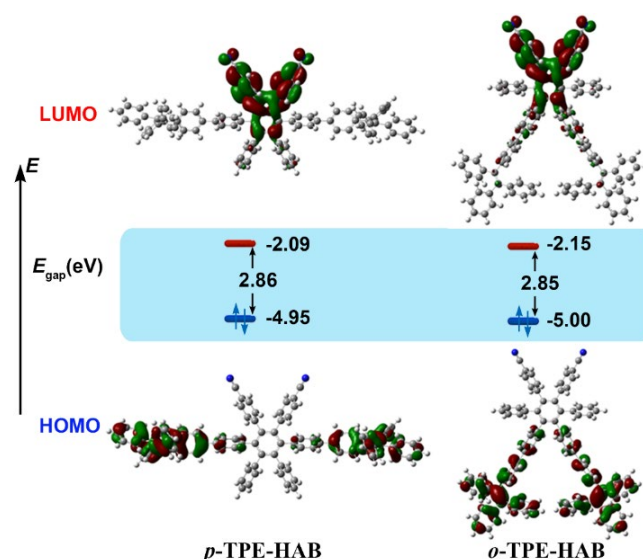


Fig. 4 Frontier-molecular-orbital distributions and energy level diagram of *p*-TPE-HAB and *o*-TPE-HAB by DFT calculations.

Experimental

General procedures

¹H NMR spectra (400 MHz) were recorded on a Nippon Denshi JEOL FT-300 NMR spectrometer with SiMe₄ as an internal reference: *J*-values are given in Hz. UV-vis spectra were recorded on a Perkin Elmer Lambda 19 UV/VIS/NIR spectrometer. Mass spectra were obtained on a Nippon Denshi JMS-01SA-2 spectrometer at 75 eV using a direct-inlet system. Gas-liquid chromatograph (GLC) analyses were performed by Shimadzu gas chromatograph, GC-14A;

silicone OV-1, 2 m; programmed temperature rise, 12 °C min⁻¹; carrier gas nitrogen, 25 mL min⁻¹.

Experimental details

1,3-Bis(4-bromophenyl)propan-2-one (1a): A solution of 4-bromophenylacetic acid (5.0 g, 23 mmol) in dichloromethane was added dropwise to a mechanically stirred solution of dicyclohexylcarbodiimide (DCC: 2.4 g, 12 mmol) and *N,N*-dimethylaminopyridine (DMAP: 0.71 g, 0.58 mmol) in dichloromethane (40 mL). The reaction was allowed to proceed overnight under an argon atmosphere at room temperature. The reaction mixture was filtered to remove dicyclohexylurea, and the filtrate was subjected to rotary evaporation. The product was purified by column chromatography with 10% ethyl acetate/hexane as eluent (2.2 g, 53% yield). ¹H NMR (400 MHz, CDCl₃): δ = 7.44 (d, *J* = 8.2 Hz, 4H), 7.01 (d, *J* = 8.1 Hz, 4H) and 3.68 (s, 4H) ppm.

2,5-Bis(4-bromophenyl)-3,4-diphenylcyclopenta-2,4-dienone (3a): A solution of KOH (0.05 g, 0.89 mmol) in ethanol (2 mL) was added dropwise into a mixture of 1,3-bis(4-bromophenyl)propan-2-one (1.0 g, 2.7 mmol) and benzil (0.57 g, 2.7 mmol) in 20 mL ethanol. The solution was refluxed for 20 min, and then cooled to 0 °C. The resulting precipitate was collected by filtration and washed with EtOH to obtain a dark crystal solid (1.30 g, yield 89%). ¹H NMR (400 MHz, CDCl₃): δ = 7.37 (d, *J* = 8.4 Hz, 4H, BrPh-*H*), 7.28 (d, *J* = 7.8 Hz, 2H, Ph-*H*), 7.19 (t, *J* = 7.5 Hz, 4H, Ph-*H*), 7.10 (d, *J* = 8.4 Hz, 4H, BrPh-*H*), 6.90 (d, *J* = 7.6 Hz, 4H, Ph-*H*) ppm.

Synthesis of compound 3b

A solution of KOH (0.05 g, 0.89 mmol) in ethanol (2 mL) was added dropwise into a mixture of 1,3-bis(4-bromophenyl)propan-2-one (1.0 g, 2.7 mmol) and benzil (0.57 g, 2.7 mmol) in 20 mL ethanol. The solution was refluxed for 20 min, and then cooled to 0 °C. The resulting precipitate was collected by filtration and washed with EtOH to obtain a dark solid (1.18 g, yield 81%). ¹H NMR (400 MHz, CDCl₃): δ = 7.34 (d, *J* = 8.5 Hz, 4H, BrPh-*H*), 7.27 (m, 6H, Ph-*H*), 7.19 (m, 4H, Ph-*H*), 6.79 (d, *J* = 7.6 Hz, 4H, BrPh-*H*) ppm.

Synthesis of compound 4a: The solution of compound **2** (360 mg, 0.66 mmol) and 4,4'-(ethyne-1,2-diyl)dibenzonitrile (152 mg, 0.66 mmol) in diphenyl ether (3 mL) was refluxed for 7 h under protection of Ar₂, and then the reaction was cooled to room temperature. The crude product was purified by column chromatography on silica gel (hexane/CH₂Cl₂, 1:2) to give the product as a light-yellow solid (414 mg yield 84%). ¹H NMR (400 MHz, CDCl₃): δ = 7.23 (d, *J* = 8.1 Hz, 4H), 7.03 (d, *J* = 8.3 Hz, 4H), 6.90 (d, *J* = 6.2 Hz, 10H), 6.76 (s, 4H), 6.63 (d, *J* = 8.3 Hz, 4H).

Synthesis of compound 4b

A solution of compound **2** (360 mg, 0.66 mmol) and 4,4'-(ethyne-1,2-diyl)dibenzonitrile (152 mg, 0.66 mmol) in diphenyl ether (3 mL) was refluxing for 7 h under protection of Ar₂, and then the reaction was cooled to room temperature. The crude product was purified by column chromatography on silica gel (hexane/CH₂Cl₂, 1:3) to give the product as a white solid (399 mg yield 81%). ¹H NMR (400 MHz, CDCl₃): δ = 7.19 (d, *J* = 8.2 Hz, 4H), 7.04 (d, *J* = 8.4 Hz, 4H), 6.91 (m, 10H), 6.76–6.71 (m, 4H), 6.66 (d, *J* = 8.4 Hz, 4H).

Synthesis of compound *p*-TPE-HAB

A mixture of **4a** (0.1 mmol, 75 mg), 4-(1,2,2-triphenylvinyl)phenylboronic acid (0.25 mmol, 115 mg), Pd(PPh₃)₄ (12 mg), toluene (10 mL) and EtOH (5 mL) were combined in a 50 mL

round-bottomed flask. K₂CO₃ (100 mg) was added to 10 mL distilled water and then poured it into the round-bottomed flask. Under nitrogen protection, the resulting reaction mixture was heated at 90 °C for 24 h. The reaction mixture was extracted, filtered and dried (MgSO₄). The reaction mixture was subject to column chromatography and recrystallization to obtain a light yellow solid in 65.1% yield (81 mg); Mp 164–165 °C; ¹H NMR (400 MHz, CDCl₃): δ = 7.19 (d, *J* = 8.3 Hz, 8H), 7.13–7.05 (m, 24H), 7.01 (m, 12H), 6.93 (d, *J* = 8.2 Hz, 4H), 6.89–6.84 (m, 8H), 6.80 (m, 8H) ppm. FAB-MS: *m/z* calcd for C₉₆H₆₄N₂ 1245.5103 [M⁺]; found 1244.5093 [M⁺].

***o*-TPE-HAB** was obtained as a white solid by column chromatographed over silica gel from CH₂Cl₂/hexane (2:1, v/v), (yield, 59.3%) using the same method as for ***p*-TPE-HAB**. Mp 154–155 °C; ¹H NMR (400 MHz, CDCl₃): δ = 7.19 (d, *J* = 8.2 Hz, 4H), 7.13–7.00 (m, 40H), 6.98 (s, 4H), 6.89 (m, 12H), 6.81–6.77 (m, 4H), 6.57 (d, *J* = 8.6 Hz, 4H); FAB-MS: *m/z* calcd for C₉₆H₆₄N₂ 1245.5103 [M⁺]; found 1244.5127 [M⁺].

Conclusions

In summary, two position-dependent hexaarylbenzene AIEgens with electron-withdrawing groups were prepared and investigated. Both AIEgens exhibited tunable emission behavior in different aggregation states, especially for their luminescence efficiency in the solid state. A competitive photoluminescence quantum yield up to 62.8% for ***p*-TPE-HAB** was obtained. Moreover, theoretical calculations indicated that the energy value of HOMOs and LUMOs for ***p*-TPE-HAB** and ***o*-TPE-HAB** are responsible for the differences in the solvatochromic effect, ICT behavior and luminescence efficiency. Overall, these results provide a novel hybridization strategy by employing different AIE units to design and construct nonplanar AIEgens

Conflicts of interest

The authors declare that they have no known competing financial interests or personal relationships that could have appeared to influence the work reported in this paper.

Acknowledgements

This work was performed under the Cooperative Research Program of “Network Joint Research Center for Materials and Devices (Institute for Materials Chemistry and Engineering, Kyushu University)”. We would like to thank the Natural Science Foundation of Shandong Province (Grant No. ZR2019BB067), this research used resources of the Advanced Light Source, which is a DOE Office of Science User Facility under contract no. DE-AC02-05CH11231. CR thanks the University of Hull for support.

Notes and references

- J. Mei, Y. N. Hong, J. W. Y. Lam, A. J. Qin, Y. H. Tang and B. Z. Tang, Aggregation-induced emission: The whole is more brilliant than the parts. *Adv. Mater.*, 2014, **26**, 5429–5479.

- 2 K. Xue, C. Wang, J. X. Wang, S. Y. Lv, B. Y. Hao, C. L. Zhu and B. Z. Tang, A sensitive and reliable organic fluorescent nanothermometer for noninvasive temperature sensing, *J. Am. Chem. Soc.*, 2021, **143**, 14147–14157.
- 3 J. Mei, N. L. C. Leung, R. T. K. Kwok, J. W. Y. Lam and B. Z. Tang, Aggregation-induced emission: Together we shine, united we soar! *Chem. Rev.*, 2015, **115**, 11718–11940.
- 4 Z. Zhao, H. K. Zhang, J. W. Y. Lam and B. Z. Tang, Aggregation-induced emission: New vistas at the aggregate level, *Angew. Chem., Int. Ed.*, 2020, **59**, 9888–9907.
- 5 P. Han, H. Xu, Z. An, Z. Y. Cai, Z. X. Cai, et al., Aggregation-induced emission, *Prog. Chem.*, 2022, **34**, 1–130.
- 6 S. Z. Li, D. P. Yan, Two-component aggregation-induced emission materials: tunable one/two-photon luminescence and stimuli-responsive switches by co-crystal formation, *Adv. Opt. Mater.*, 2018, **6**, 1800445.
- 7 T. T. Zheng, J. L. Xu, X. J. Wang, J. Zhang, X. L. Jiao, T. Wang, D. R. Chen, A novel nanoscale organic–inorganic hybrid system with significantly enhanced AIE in aqueous media, *Chem. Commun.*, 2016, **52**, 6922–6925.
- 8 J. W. Chen, Z. L. Xie, J. W. Y. Lam, C. C. W. Law, B. Z. Tang, Silole-containing polyacetylenes. synthesis, thermal stability, light emission, nanodimensional aggregation, and restricted intramolecular rotation, *Macromolecules*, 2003, **36**, 1108 – 1117.
- 9 Z. Y. Zheng, T. T. Zhou, R. Hu, M. J. Huang, X. Ao, J. Chu, T. Jiang, A. J. Qin, Z. M. Zhang, A specific aggregation-induced emission-conjugated polymer enables visual monitoring of osteogenic differentiation, *Bioact. Mater.*, 2020, **5**, 1018 – 1025.
- 10 S. S. Liow, Q. Q. Dou, D. Kai, Z. B. Li, S. Sugiarto, C. Y. Y. Yu, R. T. K. Kwok, X. H. Chen, Y. L. Wu, S. T. Ong, A. Kizhakeyil, N. K. Verma, B. Z. Tang, X. J. Loh, Long-term real-time in vivo drug release monitoring with AIE thermogelling polymer, *Small*, 2017, **13**, 1603404.
- 11 A. Gupta, P. Prasad, S. Gupta, P. K. Sasmal, Simultaneous ultrasensitive detection and elimination of drug-resistant bacteria by cyclometalated iridium(III) complexes, *ACS Appl. Mater. Interfaces*, 2020, **12**, 35967 – 35976.
- 12 H. T. Mao, Y. Yang, K. Y. Zhao, Y. C. Duan, W. L. Song, G. G. Shan, Z. M. Su, Fine-tuning emission color of aggregation-induced emission-active Ir(III) phosphors through simple ligand modification, *Dyes Pigments*, 2021, **192**, 109439.
- 13 X. Z. Yan, T. R. Cook, P. Wang, F. H. Huang, P. J. Stang, Highly emissive platinum(II) metallocages, *Nat. Chem.*, 2015, **7**, 342 – 348.
- 14 J. Luo, Z. Xie, J. W. Y. Lam, L. Cheng, B. Z. Tang, H. Chen, C. Qiu, H. S. Kwok, X. Zhan, Y. Liu, D. Zhu, Aggregation-induced emission of 1-methyl-1,2,3,4,5-pentaphenylsilole, *Chem. Commun.*, 2001, 1740–1741.
- 15 R. T. K. Kwok, C. W. T. Leung, J. W. Y. Lam, B. Z. Tang, Biosensing by luminogens with aggregation-induced emission characteristics, *Chem. Soc. Rev.*, 2015, **44**, 4228–4238.
- 16 N. L. Leung, N. Xie, W. Yuan, Y. Liu, Q. Wu, Q. Peng, Q. Miao, J. W. Y. Lam, B. Z. Tang, Restriction of intramolecular motions: The general mechanism behind aggregation-induced emission, *Chem. - Eur. J.*, 2014, **20**, 15349–15353.
- 17 L. Z. Li, M. Chen, H. K. Zhang, H. Nie, J. Z. Sun, A. J. Qin, B. Z. Tang, Influence of the number and substitution position of phenyl groups on the aggregation-enhanced emission of benzene-cored luminogens, *Chem. Commun.*, 2015, **51**, 4830 – 4833.
- 18 M. Chen, R. Chen, Y. Shi, J. G. Wang, Y. H. Cheng, Y. Li, X. D. Gao, Y. Yan, J. Z. Sun, A. J. Qin, R. T. K. Kwok, J. W. Y. Lam, B. Z. Tang, Malonitrile-functionalized tetraphenylpyrazine: aggregation-induced emission, ratiometric detection of hydrogen sulfide and mechanochromism, *Adv. Funct. Mater.*, 2018, **28**, 1704689.
- 19 F. Ren, P. Liu, Y. Gao, J. B. Shi, B. Tong, Z. X. Cai, Y. P. Dong, Real time bioimaging for mitochondria by taking the aggregation process of aggregation-induced emission near-infrared dyes with wash-free staining, *Mater. Chem. Front.*, 2019, **3**, 57 – 63.
- 20 X. Feng, X. H. Wang, C. Redshaw, B. Z. Tang, Aggregation behaviour of pyrene-based luminescent materials, from molecular design and optical properties to application, *Chem. Soc. Rev.*, 2023, **52**, 6715 – 6753.
- 21 Z. D. Yu, X. X. Dong, J. Y. Cao, W. X. Zhao, G. H. Bi, C. Z. Wang, T. Zhang, S. Rahman, P. E. Georghiou, J. B. Lin and T. Yamato, Substituent effects on the intermolecular interactions and emission behaviors in pyrene-based mechanochromic luminogens, *J. Mater. Chem. C*, 2022, **10**, 9310–9318.
- 22 J. Y. Cao, G. Yang, Z. M. Xue, W. X. Zhao, S. H. Chen, H. T. Lin, T. Yamato, C. Redshaw, D. Y. Gu, C. Z. Wang, Improved aggregation-induced emission behavior in D- π -A architectures by modifying the donor units, *Dyes Pigments*, 2023, **220**, 111758.
- 23 R. R. Hu, J. W. Y. Lam, Y. Liu, X. Zhang, B. Z. Tang, Aggregation-induced emission of tetraphenylethene–hexaphenylbenzene adducts: Effects of twisting amplitude and steric hindrance on light emission of nonplanar fluorogens, *Chem. - Eur. J.*, 2013, **19**, 5617–5624.
- 24 Z. Zhang, B. Xu, J. Su, L. Shen, Y. Xie and H. Tian, Color tunable solid-state emission of 2,2'-biindenyl-based fluorophores, *Angew. Chem., Int. Ed.*, 2011, **50**, 11654–11657
- 25 Z. F. Chang, L. M. Jing, C. Wei, Y. P. Dong, Y. C. Ye, Y. S. Zhao, J. L. Wang, Hexaphenylbenzene-based, π -conjugated snowflake-shaped luminophores: Tunable aggregation-induced emission effect and piezofluorochromism, *Chem. - Eur. J.*, 2015, **21**, 8504–8510.
- 26 Z. Li, Y. Dong, B. Mi, Y. Tang, M. Haeussler, H. Tong, Y. Dong, J. W. Y. Lam, Y. Ren, H. H. Y. Sung, K. S. Wong, P. Gao, I. D. Williams, H. S. Kwok, B. Z. Tang, Structural control of the photoluminescence of silole regioisomers and their utility as sensitive regiodiscriminating chemosensors and efficient electroluminescent materials, *J. Phys. Chem. B*, 2005, **109**, 10061–10066.
- 27 Y. Terazono, P. A. Liddell, V. Garg, G. Kodis, A. Brune, M. Hamburger, A. L. Moore, T. A. Moore, D. Gust, Artificial photosynthetic antenna-reaction center complexes based on a hexaphenylbenzene core, *J. Porphyrins Phthalocyanines*, 2005, **9**, 706–723.
- 28 H. Tong, Y. Hong, Y. Dong, M. Häußler, J. W. Y. Lam, Z. Li, Z. F. Guo, Z. H. Guo, B. Z. Tang, Fluorescent “light-up” bioprobes based on tetraphenylethylene derivatives with aggregation-induced emission characteristics, *Chem. Commun.*, 2006, 3705–3707.
- 29 J. M. Englert, J. Malig, V. A. Zamolo, A. Hirsch, N. Jux, HBC–porphyrin–close contact chromophores, *Chem. Commun.*, 2013, **49**, 4827–4829.
- 30 B. Y. Du, K. Y. Zhang, P. L. Wang, X. D. Wang, S. M. Wang, S. Y. Shao, L. X. Wang, Spirofluorene-locked carbazole based multiple resonance thermally activated delayed fluorescence emitters for efficient solution-processed narrowband green OLEDs, *J. Mater. Chem. C*, 2023, **11**, 9578–9585.
- 31 C. Z. Wang, Y. Noda, C. Wu, X. Feng, P. Venkatesan, H. Cong, M. R. J. Elsegood, T. G. Warwick, S. J. Teat, C. Redshaw, T. Yamato, Multiple photoluminescence from pyrene-fused hexaarylbenzenes with aggregation-enhanced emission features, *Asian J. Org. Chem.*, 2018, **7**, 444–450.
- 32 C. Z. Wang, Z. D. Yu, W. X. Zhao, K. Yang, Y. Noda, Y. Zhao, X. Feng, M. R. J. Elsegood, S. J. Teat, C. Redshaw, T. Yamato, Pyrene-fused hexaarylbenzene luminogens: Synthesis, characterization, and aggregation-induced emission enhancement, *Dyes Pigments*, 2021, **192**, 109452.

- 33 G. Yang, K. Y. Liu, J. Y. Cao, J. Y. Yu, D. L. Sun, C. Z. Wang, W. X. Zhao, M. R. J. Elsegood, S. J. Teat, C. C. Zhu, T. Yamato, A comparative study on optical properties of pyrene-fused [4]helicenes and vinyl precursors, *Spectrochim. Acta Part A: Mol. Biomol. Spectrosc.*, 2024, **305**, 123529.
- 34 J. Li, J. Wang, H. Li, N. Song, D. Wang, B. Z. Tang, Supramolecular materials based on AIE luminogens (AIEgens): construction and applications, *Chem. Soc. Rev.*, 2020, **49**, 1144–1172.
- 35 Q. Wang, Q. Zhang, Q. W. Zhang, X. Li, C. X. Zhao, T. Y. Xu, D. H. Qu, H. Tian. Color-tunable single-fluorophore supramolecular system with assembly-encoded emission, *Nat. Commun.*, 2020, **11**, 158.
- 36 X. L. Luo, J. N. Li, C. H. Li, L. P. Heng, Y. Q. Dong, Z. P. Liu, Z. S. Bo, B. Z. Tang, Reversible Switching of the emission of diphenyldibenzofulvenes by thermal and mechanical stimuli, *Adv. Mater.*, 2011, **23**, 3261–3265.
- 37 S. Grimme, J. Antony, S. Ehrlich, H. Krieg, A consistent and accurate ab initio parametrization of density functional dispersion correction (DFT-D) for the 94 elements H-Pu, *J. Chem. Phys.*, 2010, **132**, 154104.
- 38 J. Liu, Y. Zhang, K. Zhang, J. Fan, C. K. Wang, L. Lin. Bicolor switching mechanism of multifunctional light-emitting molecular material in solid phase, *Org. Electron.*, 2019, **71**, 212–219.